Unprecedented N–E Bond Cleavage (E = Sn, Pb) by R_4N^+ Ions (R = *n*Bu, *n*Pr): Formation, Architecture, and Multinuclear Magnetic Resonance Spectroscopy of Novel Supramolecular $[(R_4N)(Me_3E)_2M(CN)_6 \cdot H_2O]$ Assemblies (M = Fe, Co)

Peter Schwarz, Eric Siebel, R. Dieter Fischer,* Nicola A. Davies, David C. Apperley, and Robin K. Harris*

Abstract: Novel supramolecular assemblies **2** of the composition $[(n\mathrm{Bu}_4\mathrm{N})(\mathrm{Me}_3\mathrm{E})_2\mathrm{M}(\mathrm{CN})_6 \cdot \mathrm{H}_2\mathrm{O}]$ (E = Sn, Pb; M = Fe, Co) have been obtained both by spontaneous self-assembly of small ions and by exchange remodeling of the known, sparingly soluble, coordination polymers $[(\mathrm{Me}_3\mathrm{E})_3\mathrm{M}(\mathrm{CN})_6]$. Product **2a** (E = Sn, M = Fe) was characterized by single-crystal X-ray crystallography, and its diamagnetic homologue **2b** (E = Sn, M = Co) by in-depth multinuclear (^{13}C, ^{15}N, ^{59}Co, ^{119}Sn) solid-state magnetic resonance spectroscopy. The architecture of **2a** is based on slightly puckered, porous nets involving coordinative $N_{cyanide} \rightarrow Sn$ and $O_{water} \rightarrow Sn$ bonds. These nets are stacked regularly and are held together by O–H···N and (*n*Bu)*α*-C–H···N hydrogen bonds. This produces nanometer-sized channels that host two thirds of the $n\mathrm{Bu}_4\mathrm{N}^+$ ions. Unexpected $[(\mathrm{Me}_3\mathrm{Sn}(\mathrm{OH}_2)_2]^+$ ions and the remaining third of the $n\mathrm{Bu}_4\mathrm{N}^+$ ions are trapped between adjacent [-Fe-CN-Sn-NC-]$_\infty$ chains. Both the methods of formation of **2a/b** and their (probably analogous) structures are suggestive of a pronounced superiority of *concerted* O→Sn *and* D–H···N bonding (D = OH and CH_2) over an exclusive N→Sn coordination.

Keywords: hydrogen bonds · nanostructures · NMR spectroscopy · structure elucidation · supramolecular chemistry

Introduction

Coordination polymers of the composition $[(\mathrm{Me}_3\mathrm{E})_3\mathrm{M}(\mathrm{CN})_6]$ (type **1**) with E = Sn or Pb and M = Fe or Co crystallize as well-defined, voluminous 3D frameworks of infinite [-M-CN-(EMe_3)-NC-] chains with trigonal bipyramidal (tbp) $\mathrm{Me}_3\mathrm{E}(\mathrm{NC})_2$ units as M-connecting building blocks.[1] Their facile formation by spontaneous precipitation (self-assembly) from aqueous solutions containing both $\mathrm{Me}_3\mathrm{E} \cdot \mathrm{aq}^+$ and $[\mathrm{M}(\mathrm{CN})_6]^{3-}$ ions [Eq. (1)] suggests that the chain-propagating N–E bonds are energetically superior to the O–E bonds present in the $\mathrm{Me}_3\mathrm{E} \cdot \mathrm{aq}^+$ ion in solution which also has a tbp configuration.[2] Despite numerous attempts, we have not been able to synthesize insoluble supramolecular aggregates of type **2** $[\mathrm{A}(\mathrm{Me}_3\mathrm{E})_2\mathrm{M}(\mathrm{CN})_6]$, where A is a less specifically (than e.g. $\mathrm{Me}_3\mathrm{E}^+$) coordinating cation, such as K^+, Et_4N^+, or $[CoCp_2]^+$ (Cp = η^5-C_5H_5) [Eq. (2); M = Fe, Co]. Only the

$$3\,\mathrm{Me}_3\mathrm{ECl} + \mathrm{K}_3[\mathrm{M}(\mathrm{CN})_6] \xrightarrow{\mathrm{H_2O}} \underset{\text{(type 1)}}{[(\mathrm{Me}_3\mathrm{E})_3\mathrm{M}(\mathrm{CN})_6]\downarrow} + 3\,\mathrm{K}^+ + 3\,\mathrm{Cl}^- \quad (1)$$

$$\mathrm{A}^+ + 2\,\mathrm{Me}_3\mathrm{E} \cdot \mathrm{aq}^+ + [\mathrm{M}(\mathrm{CN})_6]^{3-} \xrightarrow{\mathrm{H_2O}} [\mathrm{A}(\mathrm{Me}_3\mathrm{E})_2\mathrm{M}(\mathrm{CN})_6]\downarrow \quad (\mathrm{A}^+ = \mathrm{K}^+, \mathrm{Et}_4\mathrm{N}^+, [\mathrm{CoCp}_2]^+) \quad (2)$$

corresponding type **1** system (if any) precipitated in the latter reaction. At first glance it is tempting to assume that less than six N–E bonds per formula unit might be insufficient to produce insoluble aggregates. This hypothesis is, however, questioned by the surprising fact that the formation of *hydrated* type **2** derivatives takes place in the presence of the larger (than $A = Et_4N^+$) $n\mathrm{Bu}_4\mathrm{N}^+$ ion, even if $\mathrm{Me}_3\mathrm{SnCl}$ is present in notable excess [Eq. (3); M = Fe, Co].

$$2 \text{ or } 3\,\mathrm{Me}_3\mathrm{SnCl} + n\mathrm{Bu}_4\mathrm{NCl} + \mathrm{K}_3[\mathrm{M}(\mathrm{CN})_6] \xrightarrow{\mathrm{H_2O}} [(n\mathrm{Bu}_4\mathrm{N})(\mathrm{Me}_3\mathrm{Sn})_2\mathrm{M}(\mathrm{CN})_6 \cdot \mathrm{H}_2\mathrm{O}]\downarrow + 3\,\mathrm{K}^+ + 3 \text{ or } 4\,\mathrm{Cl}^- + 0 \text{ or } 1\,\mathrm{Me}_3\mathrm{Sn} \cdot \mathrm{aq}^+ \quad (3)$$

Furthermore, if $[(\mathrm{Me}_3\mathrm{E})_3\mathrm{M}(\mathrm{CN})_6]$ (type **1**) is suspended in an aqueous solution of $n\mathrm{Bu}_4\mathrm{NCl}$ it is completely converted to a product of type **2**, which is also insoluble [Eq. (4); E = Sn,

[*] Prof. Dr. R. D. Fischer, Dr. P. Schwarz, Dipl.-Chem. E. Siebel
Institut für Anorganische und Angewandte Chemie
der Universität Hamburg
Martin-Luther-King-Platz 6, D-20146 Hamburg (Germany)
Fax: (+49) 40-4123-2893
Prof. Dr. R. K. Harris, Dr. D. C. Apperley, N. A. Davies, M.Sc.
University of Durham, Department of Chemistry
South Road, Durham, DH1 3LE (UK)
Fax: (+44) 191-386-1127

  0947-6539/98/0405-0919 $ 17.50+.25/0

$$[(Me_3E)_3M(CN)_6] + nBu_4N^+ \xrightarrow{H_2O} [(nBu_4N)(Me_3E)_2M(CN)_6 \cdot H_2O] + Me_3E \cdot aq^+ \quad (4)$$
(type **2**)

Pb; M = Fe, Co]. The products from this reaction were identical to the corresponding precipitates obtained according to Equation (3). Interestingly, throughout reaction (4), the polymeric reactant remains virtually insoluble. According to Equation (4), at least two of the six N – Sn bonds present per formula unit of **1** should be cleaved in the presence of nBu_4N^+ ions with formal compensation by the two[2] O – Sn bonds of the soluble $Me_3Sn \cdot aq^+$ ion which is also formed. To rationalize the unexpectedly high driving force of the spontaneous reactions described by Equations (3) and (4), two representatives of the novel type **2** compound $[(nBu_4N)(Me_3E)_2M(CN)_6 \cdot H_2O]$ have been investigated in more detail. The successful elucidation of the highly informative single-crystal X-ray structure of **2a** provides, amongst other things, a very promising basis for the evaluation of the multinuclear solid-state magnetic resonance study of its diamagnetic homologue **2b** (M = Co), which is probably isostructural. The real architecture of **2a**, presumably unpredictable from first principles, suggests, in agreement with the NMR results for **2b**, that additional *hydrogen bonds* of the type O–H ··· N and C–H ··· N play a key role in the unexpected restructuring process described by Equations (3) and (4).

Results and Discussion

General properties of 2a – 2f: We used the two routes mentioned in the Introduction [route A: coprecipitation according to Equation (3); route B: remodeling of a suspended type **1** system according to Equation (4)], to prepare four different homologues of type **2** [M = Fe, Co; R = *n*Bu; E = Sn or Pb (**2a – 2d**, see Table 1)]. The designations **1a – d** follow the specifications in columns 3 and 4 of Table 1. Although the counteranion X^- of the reactant R_4NX of route B was varied (Table 1), no significant influence of X^- on the course of the reaction was observed. It may, however, be noted that all Fe^{III} was reduced by $X = BH_4^-$ to afford the host – guest system $[(nBu_4N)_{0.5}(Me_3Sn)_{3.5}Fe(CN)_6 \cdot H_2O]$ (with E = Sn) already reported.[3] To indicate that, again in sharp contrast to our experience with $A = Et_4N^+$ (vide supra), type **2** systems with R = *n*Pr are also available, the first two examples of this subclass (**2e** and **2f**) are also included in Table 1. The presence of nonremovable H_2O molecules (at least after prolonged drying in vacuo) in all the products was confirmed by the elemental analyses which included oxygen (vide infra) and by relatively intense, and sharp, respectively, ν(OH)- and δ(OH) absorptions in the IR spectra (i.e. 3400 – 3150 cm^{-1} and 1628 – 1634 cm^{-1}). All type **2** systems are readily soluble in D_2O/NaOD, and the ^1H NMR spectra of the resulting solutions provided independent confirmation of the presence of the ions R_4N^+ and Me_3E^+ in the expected ratio 1:2. The paramagnetic Fe^{III} compounds (μ_{eff} of **2a**: 1.85 B.M.) are, like **1a** and **1c**,[1] sensitive to light and even weak reducing agents. Thus, irradiation of **2a** (150 W xenon lamp, 1.5 h) led to a dirty-greenish product with the main ν(CN) absorption at 2054 cm^{-1} (instead of ν(CN) = 2131 cm^{-1} for pristine **2a**, see Table 2). When **2c** was subjected to an atmosphere enriched with pyrrole vapor, a black, polypyrrole-containing composite **3c** resulted. The electrical conductivity of **3c** at 300 K (3.33×10^{-3} S cm^{-1}) exceeds that of **2c** ($\approx 10^{-7}$ S cm^{-1}) by four orders of magnitude.[4] Similar observations have been made on the exposure of **1a** and **1c** to pyrrole.[5] In an atmosphere of aniline, yellow **2a** converted into a dark green solid which contained both Fe^{II} and Fe^{III}.[4]

Although **2a – 2d**, unlike **1a** and **1b**, should contain both bridging (to E atoms) and *non*bridging (i.e. virtually terminal)

Table 1. Survey of the new products $[(R_4N)(Me_3E)_2M(CN)_6 \cdot x H_2O]$ ($x = 1$ for **2a – d** and 2 for **2e** and **2f**). The notations **1a – d** follow the items given in columns 3 and 4.

Product	R	E	M	Route (anion)
2a	*n*Bu	Sn	Fe	A; B (OH)
2b	*n*Bu	Sn	Co	A; B (Br, Cl)
2c	*n*Bu	Pb	Fe	A; B (BF_4)
2d	*n*Bu	Pb	Co	B (OH)
2e	*n*Pr	Sn	Fe	B (Cl)
2f	*n*Pr	Sn	Co	B (Cl)

Table 2. ν(CN) frequencies (cm^{-1}) of several type **2** systems at different temperatures.

2a		**2b**		**2c**	**2d**	**2e**
RT[a]	LT[b]	RT[a]	LT[b]	RT[a]	RT[a]	RT[a]
		2173[c]	2177			
	2154	2157[c]	2153			2158
2131 br[d]	2138	2141 br[e]	2145	2134	2143	2135
	2123		2133	2121	2123	
	2119			2116	2119	2092 w
	2075			2104		2051 w
	2027					

[a] Room temperature. [b] Liquid nitrogen temperature. [c] Raman spectrum (RT). [d] ν(CN) absorption of **1a**: 2140 cm^{-1}. [e] ν(CN) absorption of **1b**: 2158 cm^{-1}.

Abstract in German: *Neuartige supramolekulare Aggregate der Zusammensetzung [(nBu4N)(Me3E)2M(CN)6 · H2O] (E = Sn, Pb; M = Fe, Co) entstehen sowohl bei der spontanen Selbstorganisation einfacher Ionen als auch durch Ionenaustausch aus den schon bekannten, schwerlöslichen Koordinationspolymeren [(Me3E)3M(CN)6]. Die Verbindung **2a** (E = Sn, M = Fe) wurde röntgenstrukturanalytisch und ihr diamagnetisches Homologes **2b** (E = Sn, M = Co) durch Mehrkern-Festkörper-NMR-Spektroskopie (13C, 15N, 59Co, 119Sn) ausführlich charakterisiert. Das Gitter von **2a** besteht aus weitporigen, leicht gewellten Netzen mit NCyanid → Sn- und OWasser → Sn-Verknüpfung, deren Stapelung nanometergroße Kanäle erzeugt, welche zwei Drittel aller nBu4N+-Ionen aufnehmen. Zwischen zwei Ketten benachbarter Netze befinden sich unerwarteterweise [Me3Sn(OH2)2]+- und die restlichen nBu4N+-Ionen. Sowohl die Art der Entstehung von **2a/b** als auch ihre (vermutlich gleichen) Strukturen sprechen für eine deutliche Überlegenheit der hier konzertiert auftretenden O → Sn- und D–H ··· N-Bindungen (D = OH und CH2) über ausschließlich koordinative N → Sn Bindungen.*

0947-6539/98/0405-0920 $ 17.50+.50/0 *Chem. Eur. J.* **1998**, *4*, No. 5

CN ligands, the room-temperature IR spectra of **2a** and **2b** display (in contrast to those of **2c**–**2e**) only *one* symmetrical, but comparatively broad, ν(CN) band. However, at least four individual ν(CN) bands became reversibly apparent when samples of **2a** and **2b** were cooled down to liquid nitrogen temperature (Table 2). The room-temperature Raman spectrum of **2b** exhibits at least four ν(CN) bands. There is only one IR-active ν(EC) band in the spectra of **2a,b** (555 cm^{-1}) and **2c,d** (498 cm^{-1}). The Raman spectra always show two ν(SnC) bands (for example: **2b**: $\nu = 524$ and 558 cm^{-1}.)

All the new products (including **3c**) were microcrystalline and their X-ray powder diffractograms (XRPs) display comparatively sharp reflection lines. While the XRPs of **2a** and **2b** look very similar, significant differences between the XRPs of, for example, **2b** ($A = nBu_4N^+$) and **2f** ($A = nPr_4N^+$) suggest that the size of the templating guest ion A^+ exerts a notable structure-directing influence.

The thermal stability of the compounds (TG/DTG measurements) was found to differ: **2a** already turned black above 155 °C, while **2b** started to decompose at ≈200 °C and lost ≈ 55 % of its initial weight between 230 and 300 °C to produce a deep blue solid foam. Broad absorptions at $\lambda = 550$ and 600 nm suggest the presence of Co^{II} in the final product, while the IR spectrum (ν(CN) = 2138 cm^{-1}) remained surprisingly similar to that of **2b**. Mass spectrometric results indicated that Me_3SnCN was liberated, but a more detailed study is necessary for a comprehensive description of this unusual thermolysis.[6]

Crystal structure of 2a: The complete structural analysis of **2a** revealed that the asymmetric unit involves eight different Sn sites and three crystallographically nonequivalent nBu_4N, $Fe(CN)_6$, and H_2O components. While two of the three H_2O molecules (O3 and O4) coordinate the nonequivalent, terminal Sn atoms of chain II (see Figure 1) of the host framework, the third H_2O molecule belongs to a tbp-configured $\{Me_3Sn(OH_2)_2\}^+$ cation (containing symmetry-related water molecules) which was found to be a completely unexpected, second guest cation of a structurally quite complex host–guest system. A more transparent description of this system requires at least three formula units: $\{3 \times \mathbf{2a}\} = [(nBu_4N)_3\ \{Me_3Sn(OH_2)_2\}_{0.5}\ \{(Me_3Sn)_{5.5}(H_2O)_2Fe(CN)_6\}_3]$.
guest 1 guest 2 host framework
Interestingly, the crystal structure of **2a** indicates that the reaction described by Equation (4) actually involves the cleavage of *three* (rather than two, vide supra) N–Sn bonds per formula unit, with concomitant formation of one O–Sn bond *within* the new solid. The negatively charged host framework consists of the infinite chain I: [-Fe1-C13-N13-Sn5-N13′-C13′-Fe1′-C16-N16-Sn6-N16′-C16′-]$_\infty$ (chain I) and of the finite chain II: {O3-Sn3-N36-C36-Fe3-C35-N35-Sn2-N22-C22-Fe2-C23-N23-Sn4-O4} (chain II).

As is shown schematically in Figure 1, each Fe1 atom of chain I is connected to an Fe2 atom of chain II by a $(CN)_2Me_3Sn1$ tether, and all Fe3 atoms of adjacent type II chains are also interlinked pairwise by $(CN)_2Me_3Sn7$ bridges. Each of the three types of iron atoms (Fe1, Fe2, and Fe3) is coordinated to three bridging CN ligands (to Sn atoms) and to three virtually nonbridging CN ligands, both with *meridional*

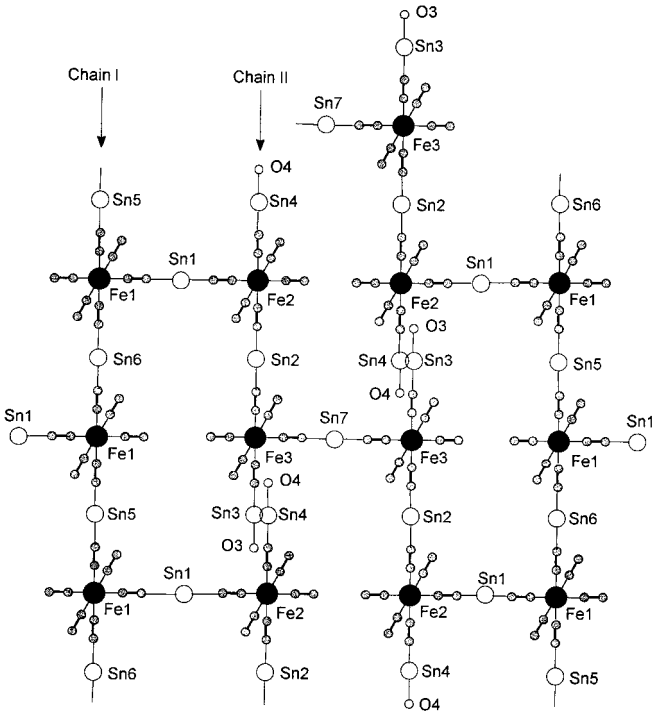

Figure 1. Schematic presentation of one of the porous layers of **2a**. Both chains (I and II) extend vertically, and the two guest ions have been omitted for clarity.

configurations. Such *mer*-$\{Fe(CNSn)_3(CN)_3\}$ units should at least give rise to two reasonably intense, IR-active ν(CN) bands characteristic of bridging cyanide, and also to two IR-active ν(CN) bands more typical of terminal cyanide ligands.[7] Hence, in the absence of any further differences between the three crystallographically nonequivalent $\{Fe(CN)_6\}$ units, the expectation of about four comparatively intense ν(CN) bands (vide supra) would in fact be reasonable.

Only one half of the eighteen nonequivalent $N_{cyanide}$ atoms per unit cell is bonded to Sn atoms (Table 3). The comparatively long[8] Sn–N bond length of ≈230 pm is in good

Table 3. Bond lengths (pm) and angles (°) of all the nonequivalent Sn-N-C fragments present in **2a**.

triatomic fragment[a]	Sn–N distance	Sn-N-C angle
Sn1-N14-C14	228.0(11)	168.5(11)
Sn1-N24-C24	235.8(10)	143.0(11)
Sn2-N22-C22	232.8(11)	152.8(12)
Sn2-N35-C35	231.4(11)	156.6(12)
Sn3-N36-C36	226.3(9)	173.2(10)
Sn4-N23-C23	228.0(11)	161.1(13)
Sn5-N13-C13	233.9(10)	145.8(10)
Sn6-N16-C16	232.2(11)	156.6(13)
Sn7-N31-C31	234.4(15)	157.7(11)

[a] The first digit following the C or N symbol refers to the numbering of the Fe atom carrying those CN ligands.

agreement with that reported for polymeric metal cyanides.[9] Most of the Sn-N-C angles of **2a** differ notably from 180° (Table 3). The three individual Sn–O distances in **2a** (Table 4) deviate neither markedly from the Sn–N distances nor from the Sn–O contacts reported for the 3D framework systems $[(Me_3Sn)_4Fe(CN)_6 \cdot 2H_2O \cdot C_4H_8O_2]$, **4** (229.5 and

Table 4. Sn – O, N ··· O, and N ··· C distances in the lattice of **2a** (the latter two distances result from hydrogen bonding).

Sn – O and N ··· O contacts		N ··· C contacts (< 350 pm)[a]	
Sn3 – O3	236.3(7)	N11 ··· C609	336.62(8)
Sn4 – O4	231.0(8)	N12 ··· C401	337.36(8)
Sn8 – O8[b]	230.8(9)	N12 ··· C409	317.32(7)
		N25 ··· C505	317.87(7)
N11 – O4	264.9(6)	N25 ··· C513	342.98(8)
N15 – O8[b]	271.8(7)	N26 ··· C613	318.83(7)
N21 – O8[b]	280.2(1)	N32 ··· C405	329.90(8)
N26 – O3	269.1(2)	N32 ··· C413	348.44(8)
N32 – O4	267.0(2)	N33 ··· C501	343.69(8)
N34 – O3	278.7(0)	N34 ··· C509	326.17(7)

[a] Somewhat longer N ··· C contacts are 358.72(8), 383.39(9), and 384.04(9) pm for N26 ··· C605, N11 ··· C601, and N15 ··· C601, respectively. [b] O8 belongs to the $[Me_3Sn(OH_2)_2]^+$ guest ion.

232.6 pm[10]) and $[(Me_3Sn)_4Fe(CN)_6 \cdot 4H_2O]$, **5** (235.0 pm[11]), but are shorter than in the 3D polymer $[(nBu_4N)_{0.5}(Me_3Sn)_{3.5}Fe(CN)_6 \cdot H_2O]$, **6** (266.4 pm[3]). The Sn8 – O8 distance in the $[Me_3Sn(OH_2)_2]^+$ guest ion of **2a** matches well with the Sn – O distances reported for the ion pair $[Me_3Sn(OH_2)_2][N(SO_2Me)_2]$ (225.4 and 232.7 pm[12]).

A perspective of the experimentally determined structure of **2a**, viewed along its crystallographic *a* axis, is presented in Figure 2. This arrangement has some resemblance to the

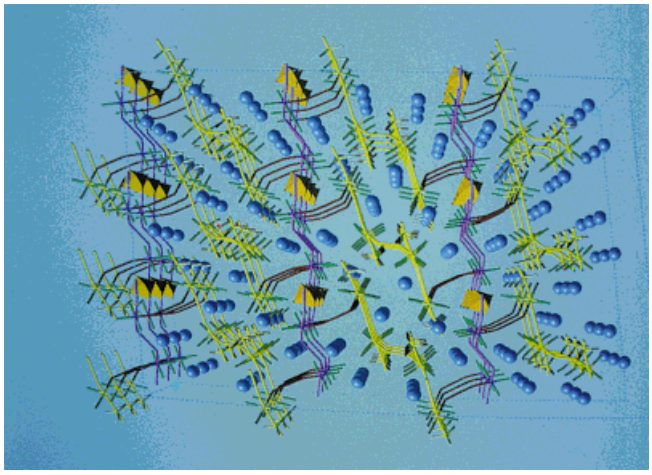

Figure 2. Perspective of the crystal structure of **2a** viewed along the *a* axis. As in Figure 1, chains I and II extend almost vertically; for further explanation see the text.

schematic description given in Figure 1. Wine-red lines indicate chains of type I and yellow lines chains of type II; all terminal cyanide ligands are marked in green. Only the methyl groups of the terminal Sn3 and Sn4 atoms (of chain II) are shown, while all other Sn-bonded methyl groups have been omitted for clarity. Similarly, only the N atoms of the nBu_4N^+ ions are shown as large blue spheres, while the $[Me_3Sn(OH_2)_2]^+$ ions are presented as brown trigonal bipyramids. Interestingly, only two of the three nonequivalent nBu_4N^+ ions are located in the interior of the two different channels extending along *a*. The third nBu_4N^+ ion (containing N5) and the $[Me_3Sn(OH)_2)_2]^+$ guest ion are predominantly located within the channel walls between two adjacent chains of the same type. Another perspective (Figure 3), in which the

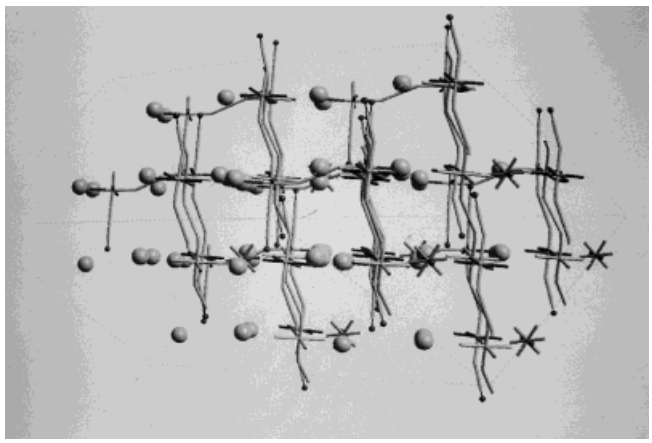

Figure 3. Perspective of the crystal structure of **2a** with practically coinciding chains I and II. Large spheres: N of nBu_4N^+; small spheres: O of H_2O.

projections of chain I and chain II virtually coincide, discloses infinite channels of an approximately quadratic cross section of $\approx 1.0 \times 1.0$ nm (measured between the *centers* of the relevant atoms). These channels are reminiscent of those present in the framework structure of **1b**[1] and are only partially filled by alkyl groups (i.e. *n*Bu and Me). This latter perspective also indicates that the basic host framework of **2a** is essentially lamellar, the projections of these layers extending vertically in Figure 3.

While, in spite of the notable Sn-N-C bending, none of the bridging (to Sn) N atoms takes part in any hydrogen bonding, six of the nine virtually terminal N atoms are involved in O–H ··· N hydrogen bridges to water molecules. The corresponding O ··· N distances (Table 4) are considerably shorter than the shortest O ··· N contacts which have been observed, for example in **4** (312.2 pm[10]) and in **5** (305.2 and 297.2 pm[11]). The O–H ··· $N_{cyanide}$ bridges with O ··· N distances ranging between 280 and 295 pm are, however, well-known for numerous salt hydrates, for example the dihydrated cyanoelpasolites $[(NMe_4)_2LiM(CN)_6 \cdot 2H_2O]$ (M = Fe,Co[13]).

In addition, seven of the nine virtually terminal cyanide ligands of **2a** exhibit at least one notably short (i.e. < 350 pm) N ··· *C* contact (Table 4) owing to potential C–H ··· N hydrogen bridges with some of the satisfactorily "acidic" α-methylene groups of the nBu_4N^+ cations.[14] Three of the terminal N atoms (N12, N25, and N33) seem to be exclusively involved in C–H ··· N interactions (Table 4), while corresponding C–H ··· O bridges do not exist in **2a**. Some of the C ··· N contacts (i.e. those shorter than 320 pm) are amongst the shortest ones of this category so far reported,[14] and it is tempting to suspect that these C–H ··· N hydrogen bridges may be essential for the particular architecture of the type **2** aggregates. Actually, the structure of **2a** would remain lamellar as long as its hydrogen bonds are ignored (vide supra); but if the latter are also taken into account then a veritable three-dimensional framework emerges.

Solid-state NMR spectroscopy of 2b: Figure 4 demonstrates that the XRP of crystalline **2a**, as calculated from its single-crystal X-ray data, resembles not only the experimental XRP of bulk **2a**, but also of diamagnetic **2b**. Hence, in view of the

0947-6539/98/0405-0922 $ 17.50+.50/0 *Chem. Eur. J.* **1998**, *4*, No. 5

unfavorable paramagnetic nature of **2a**, we have subjected its potentially isostructural, diamagnetic cobalt^{III} homologue **2b** to a detailed multinuclear CPMAS solid-state magnetic resonance investigation. In principle, **2b** is a promising candidate for ^{13}C, ^{15}N, ^{119}Sn, *and* ^{59}Co NMR spectroscopy. In order to improve the quality of the $^{15}N_{cyanide}$ NMR spectra, a sample of **2b** considerably enriched in $^{15}N_{cyanide}$ (ca. 50 %) was also prepared and included in our studies.

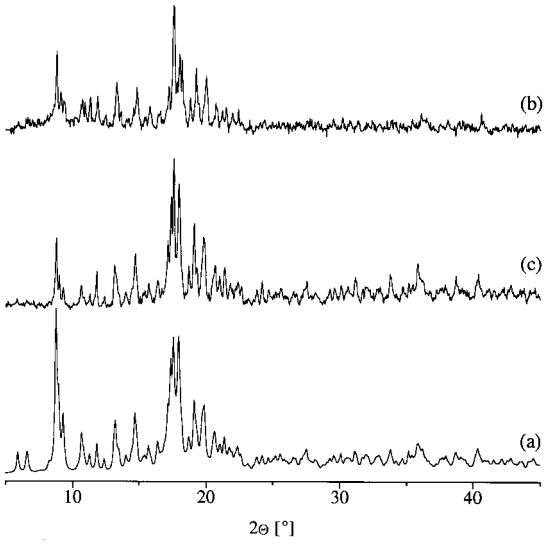

Figure 4. X-ray powder diffractograms of a) **2a** (simulated), b) **2b** (experimental), and c) **2a** (experimental).

In accordance with the X-ray structure of **2a** with its four slightly modified kinds of tbp-configured Me_3Sn features which have axial fragments with O-Sn-O (for Sn8 only), O-Sn-N (for Sn3 and Sn4), N-Sn-N′(for Sn1 and Sn2), and N-Sn-N (for Sn5, Sn6, and Sn7), a similar variety might also be expected for **2b**, and should be reflected in the ^{119}Sn NMR spectrum by a corresponding centerband pattern. The last two types of environment mentioned are, however, very similar, because in the N-Sn-N′ fragment only the Sn-N-C angles may differ (Table 3). Experimentally, three distinct resonance ranges can be recognized immediately (Figure 5): one particularly sharp, and fairly isolated, singlet at $\delta = +21.5$ should be assigned to Sn8, because the reported ^{119}Sn resonance of $[Me_3Sn(OH_2)_2][N(SO_2Me)_2]$ is positive ($\delta = +37.3$[15]). There is a relatively narrow group of lines between $\delta = -66$ and -73, and a third group of three lines of differing intensities is found between $\delta = -105$ and -123. While Sn3 and Sn4 are, in view of our earlier experience with the O-Sn-N fragment,[16] expected to resonate above $\delta = -100$, the ^{119}Sn shifts of the N-Sn-N′ *and* N-Sn-N, groups may appear either above or below this value. Ignoring the very weak centerband at $\delta = -121.5$ (as a potential impurity), there appear to be two tin signals at $\delta = -115$ and -108, arising from the N-Sn-N groups (but it is not possible to assign these individually). Between $\delta = -66$ and -73, there seem to be six resolved or partly resolved lines although five are expected (including those from O-Sn-N groups) from the structure as determined by X-ray diffraction. We believe this modest discrepancy probably arises either from quadrupolar effects from ^{59}Co (or even ^{14}N, given that the enriched sample only contains 50 % ^{15}N) or from a partial disorder of the Sn atoms in **2b** (or possibly from an impurity).

As is usually observed at ambient temperature, we assume rapid (on the NMR time scale) rotation of all Me_3Sn groups about their trigonal axes, so that only eight ^{13}C resonances would be expected for the twenty-four crystallographically different (at least in the case of **2a**) Sn-bonded *methyl* carbon atoms. However, only five distinct ^{13}C resonances of Sn-bonded Me groups are detectable at room temperature, although deconvolution of the methyl carbon resonance range actually leads to eight individual lines at $\delta = 1.9$, 1.6, 1.5, 1.4, 0.7 (two lines), 0.0 and -0.2 (with an apparent intensity range over a factor of 2). We are not aware of any polymeric metal cyanides containing Me_3Sn units which do not rotate at room temperature.[17] Furthermore, the significant overlapping of peaks in the region of the methyl carbon resonances of **2b** would make the appearance of more than eight distinct lines (at sufficiently low temperatures) difficult to observe.

While the three nonequivalent nBu_4N^+ guest ions give rise to only one ^{15}N singlet at $\delta = -309$, the *n*Bu-carbons in the α-, β-, γ-, and δ-positions show four distinct, but faintly structured, clusters of resonance lines (Figure 6). Crystallographically, the *n*Bu groups of **2a** are in fact somewhat disordered.

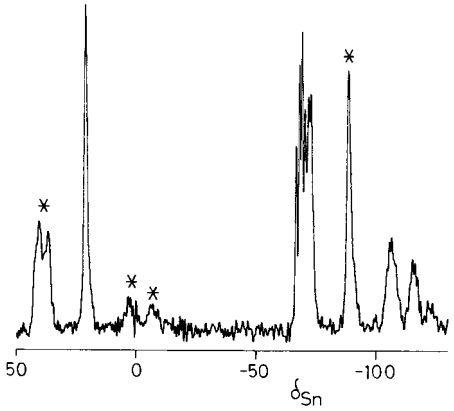

Figure 5. ^{119}Sn CPMAS spectrum of **2b**. Only the centerband region is shown with spinning sidebands marked ∗. Acquisition conditions: recycle delay 2 s, contact time 9 ms, 29500 transients, spin rate 12.2 kHz.

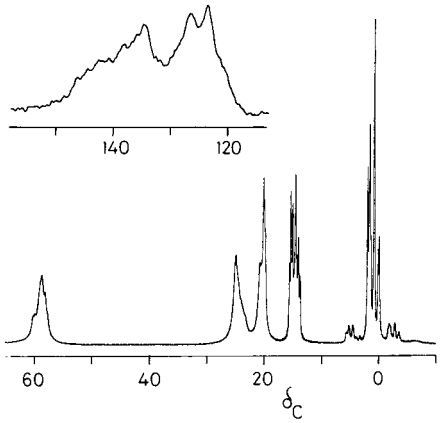

Figure 6. ^{13}C CPMAS spectrum of **2b**. The low-frequency region is shown with the CN centerband as an inset. The acquisition conditions used were a recycle delay of 1 s, contact time of 9 ms, 55000 transients, and a spin rate of 4.7 kHz.

While the band for the α-methylene carbon atoms at $\delta \approx 59$ displays little or no fine structure, the band for the terminal δ-methyl groups exhibits eight distinct lines and can be deconvoluted into a group of twelve closely lying singlets. Four blocks of twelve individual lines would be in absolute agreement with the structural findings for **2a**.

Very satisfactory agreement with the crystal structure of **2a** was found for the $^{15}N_{cyanide}$ spectrum of ^{15}N-enriched **2b** (Figure 7 and Table 5). A comparison with the spectrum of a non-^{15}N enriched sample reveals that only the notably improved signal-to-noise ratio of the ^{15}N-enriched sample guarantees unambiguous identification of the genuine center-bands. The seven almost equally intense lines between $\delta = -114$ and -131 as well as the singlet at $\delta = -121.9$ (which is about twice as intense) can be assigned to the nine non-equivalent N atoms bonded to Me_3Sn groups. N atoms of bridging CN ligands usually resonate at lower frequencies than terminal ones.[1, 16] Considering the signal at $\delta = -92.3$ as twice as intense as the four other resonances between $\delta = -88$ and -95, this subgroup could be best ascribed to the six N atoms engaged in O–H···N hydrogen bonds (vide supra). The remaining two relatively broad singlets at $\delta = -70.7$ and -73.6, with relative intensity 1:2, should then correspond to the three, virtually terminal CN ligands exclusively involved in rather weak C–H···N hydrogen bonding. In view of the C–H···N distances (Table 4), it is tempting to assign the line at $\delta = -71$ to N33 and that at $\delta = -74$ to N12 and N25 (by accidental coincidence). Interestingly, the $^{15}N_{cyanide}$ resonance of solid $[Et_4N]_3[Co(CN)_6]$ is displaced to a notably *lower* frequency ($\delta = -89.8$[1]), although its virtually terminal CN ligands would only be capable of taking part in C–H···N bonding. The actual *number* of C–H···N interactions per CN unit is, however, unknown.

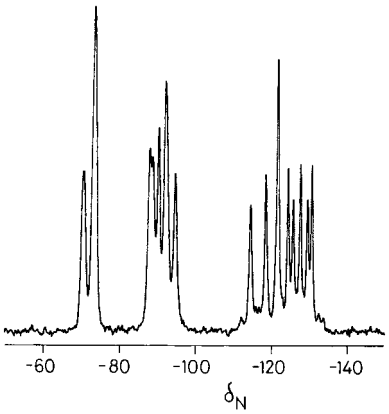

Figure 7. ^{15}N CPMAS spectrum of ^{15}N-enriched **2b**. Acquisition conditions: recycle delay 2 s, contact time 9 ms, 4000 transients, spin rate 4.7 kHz.

Table 5. $^{15}N_{cyanide}$ chemical shifts for the ^{15}N-enriched sample of $[(n-Bu_4N)(Me_3Sn)_2Co(CN)_6 \cdot H_2O]$ **2b**.

Type of nitrogen	$\delta(^{15}N)$	Number[a]
virtually terminal, –C≡N:	–70.7, –73.6[b]	12, 25, 33
hydrogen-bonded, –C≡N···H–O	–88.2, –88.9, –90.5, –92.3[b], –94.9	11, 15, 21, 26, 32, 34
metal-bridging, –C≡N→Sn	–114.7, –118.7, –121.9[b] –124.6, –126.0, –127.9 –129.7, –130.9	13, 14, 16, 22, 23, 24, 31, 35, 36

[a] Of the various nitrogen atoms of **2a** (see Table 4); individual assignments remain uncertain. [b] Two overlapping lines.

The above results underscore the usefulness of solid-state ^{15}N NMR spectroscopy as a tool for structural elucidation. Thus, we have recently discovered that ^{15}N-enriched **1d** displays, in contrast to the nonenriched sample already described,[1] *six* different $^{15}N_{cyanide}$ resonances (at $\delta = -112.4$, -117.8, -119.1, 122.1, -123.4, and -124.2). This number of signals agrees perfectly with the crystallographically deduced space group $P2_1/c$ (and not $C2/c$) of **1d**.[1] While, again in accordance with the space group $P2_1/c$, *three* methyl ^{13}C resonances (of rapidly rotating Me_3Pb units) were found, both the ^{119}Sn and the ^{59}Co spectra consist of only two and one signal(s), respectively, instead of (for $P2_1/c$) three and two lines.[1] On the other hand, ^{15}N NMR spectra may be particularly sensitive to ^{15}N-containing impurities. For instance, the room-temperature ^{15}N NMR spectrum of the (analytically appropriate) host–guest system $[(n-Bu_4N)_{0.5}(Me_3Sn)_{3.5}Fe(CN)_6 \cdot H_2O]$ (**6**[3]) obtained from $[(Me_3Sn)_4Fe(CN)_6]$ (enriched in ^{15}N to ca. 99%) by ion exchange also displayed the three ^{15}N resonances of the latter polymer, while only the five signals of authentic **6** (enriched in ^{15}N to ca. 50%) were observed when its preparation had been carried out by coprecipitation.[18]

The cyanide carbon atoms of **2b** give rise to a broad band between $\delta \approx 120$ and 145 (Figure 5). As **1b** and **1d** are known to display (relatively broad) resonances between $\delta = 132$ and 135, the somewhat wider resonance range of **2b** seems to reflect the presence of both bridging and virtually terminal cyanide ligands. The strong crowding and overlapping of the (18 expected) cyanide ^{13}C lines is obviously due to the generally narrower ^{13}C-resonance range (than e.g. the $^{15}N_{cyanide}$ range), and to the high nuclear quadrupole moment of the adjacent ^{59}Co nucleus. Usually, *iron* cyanides display more resolvable ^{13}C patterns.[16]

The ^{59}Co NMR spectrum of **2b** is a complex band with several maxima which are not fully resolved. It seems to be consistent with the existence of three crystallographically nonequivalent cobalt atoms, but with some additional splittings which may arise from second-order quadrupolar effects. Table 6 presents a survey of ^{59}Co NMR data of solid samples

Table 6. ^{59}Co NMR data for various solid samples containing a $[Co(CN)_6]^{3-}$ unit.

Compound	$\delta(^{59}Co)$	Half width [Hz]	Reference
$[(Et_4N)_3Co(CN)_6]$	208	1040	[1]
$[(n-Bu_3Sn)_3Co(CN)_6]$	206	2500	[1]
$[(n-Bu_4N)(Me_3Sn)_2Co(CN)_6 \cdot H_2O]$[a] (**2b**)	–9; –24	≤1000	present work
$[(Et_3Pb)_3Co(CN)_6]$	–33	ca. 2500	present work
$[(n-Bu_4N)(Me_3Sn)_2Co(CN)_6 \cdot H_2O]$[a] (**2b**)	–63; –84	≤1000	present work
$[(Me_3Pb)_3Co_{0.5}Fe_{0.5}(CN)_6]$[b]	–148	1050	present work
$[(n-Bu_4N)(Me_3Sn)_2Co(CN)_6 \cdot H_2O]$[a] (**2b**)	–140; –159	≤1000	present work
$[(Me_3Pb)_3Co(CN)_6]$	–157	800	[1]
$[\{Me_2Sn(CH_2)_3SnMe_2\}_{1.5}Co(CN)_6]$	–211	10100	[18]
$[(Et_3Sn)_3Co(CN)_6]$	–239	345	present work
$[(Me_3Sn)_3Co(CN)_6]$	–244	560	[1]
$[H_3Co(CN)_6]$	–258	1650	[1]

[a] ^{15}N-enriched sample. [b] Paramagnetic sample.

0947-6539/98/0405-0924 $ 17.50+.50/0 *Chem. Eur. J.* **1998**, *4*, No. 5

relevant to the present study. All the ^{59}Co shifts given in this table are referred to an aqueous solution (0.26 M) of $K_3[Co(CN)_6]$ as an external standard involving O–H···N hydrogen bonds of an unknown number (per CN group). Negative δ values should indicate even stronger Co–CN···Sn or CN···H···NC interactions than in aqueous solution.

Conclusions

According to Equation (4), the net balance for the formation of **2a** is the cleavage of three Sn–N bonds and concomitant generation of three Sn–O bonds (only one of which is found *within* the new polymer **2a**) per formula unit of **1a**. In view of the experimental evidence that the Sn–$N_{cyanide}$ bonds of **1** may be considered as enthalpically slightly superior at least to Sn–O_{water} bonds (vide supra; otherwise the well-known, *spontaneous* formation of anhydrous type **1** systems by coprecipitation[1] would not take place), it is noteworthy that, again per formula unit of **2a**, two O–H···N and three to four C–H···N hydrogen bridges are also generated. Although interactions of the latter bridging mode are even weaker than hydrogen bridges between *two* notably electronegative atoms, we have demonstrated recently[14] that rather short C–H···N bridges may nevertheless be essential for the actual architecture of the host–guest system $[(CoCp_2)(Me_3Sn)_3Fe(CN)_6]$.[20] Another point of relevance is that both $[CoCp_2]^+$ and nBu$_4$N$^+$ salts are readily soluble in water owing to the presence of an unknown number of C–H···O hydrogen bonds. For a serious net balance, the number of abandoned C–H···O interactions would also have to be taken into account.

Previously reported examples of coordination polymers containing R_3Sn and with at least one virtually terminal cyanide ligand (per transition metal atom) are $[(n\text{Bu}_4\text{N})_2\{(Me_3Sn)_2OH\}_2\{Ni(CN)_4\}_2]$ (**7**[14]) and $[(Ph_3Sn)_3Fe^{III}(CN)_6\cdot H_2O\cdot 2\,MeCN]$ (**8**[21]). In both systems, one terminal CN group is also involved in substantial O–H···N hydrogen bonding. While **7** has, moreover, been shown[14] to also involve C–H···N hydrogen bonds corresponding to those found in **2a**, the formation of **8** instead of the initially expected, *anhydrous* type **1** system $[(Ph_3Sn)_3Fe(CN)_6]$ was tentatively explained by the high steric bulk of the tin-bonded phenyl groups.[21] So far, the structure of **8** has not been inspected for significant C–H···N hydrogen bonds. Nonpolymeric complexes with terminal CN ligands and {ClSn(Me$_3$)NC} units with a tbp configuration were, on the other hand, obtained from Ph_3SnCl and $[N(PPh_3)_2][Ag(CN)_2]$ and $[N(PPh_3)_2][Pd(CN)_4]$, respectively, in an organic solvent.[22]

We have previously observed that various type **1** polymers readily undergo either partial or complete $\{M(CN)_6\}^{3-}$ exchange if suspended in aqueous solutions containing $[M'(CN)_6]^{3-}$ ions (with M ≠ M′).[23] This interesting feature suggests that, in accordance with the experimental findings reported above, at pH ≤ 7 most polymers containing R_3Sn fragments are involved in rapid equilibria with soluble organotin species, for example Equations (5) and (6).

$$\{\cdots M-CN\rightarrow Sn\leftarrow NC-M\cdots\} \underset{-H_2O}{\overset{+H_2O}{\rightleftharpoons}} \{\cdots M-CN\}^- + \{H_2O\rightarrow Sn\leftarrow NC-M\cdots\}^+ \quad (5)$$

$$\{H_2O\rightarrow Sn\leftarrow NC-M\cdots\} \underset{-H_2O}{\overset{+H_2O}{\rightleftharpoons}} \{Me_3Sn(OH_2)_2\}^+ + \{NC-M\cdots\}^- \quad (6)$$

While, at pH > 7, the stronger Lewis base OH$^-$ usually leads to complete dissolution of the respective coordination polymer, at pH ≈ 7 cations capable of acting as suitable proton donors for hydrogen bonds may help to stabilize fragments with one or more nonbridging CN ligands which would otherwise only occur as intermediates, as in Equation (7). The

$$\{\cdots M-CN\}^- + \{H-Z\}^+ \rightleftharpoons \{\cdots M-CN\cdots H-Z\}\downarrow \quad (7)$$

($\{H-Z\}^+$ = e.g. $\{H_2O\rightarrow Sn\leftarrow NC-M\cdots\}^+$, $\{Me_3Sn(OH_2)_2\}^+$, or R_4N^+)

new crystalline polymers of type **2** might thus be considered as accidentally frozen-in assemblies of intermediates such as those occurring in Equations (5), (6), and (7). Although so far nBu$_4$N$^+$ and nPr$_4$N$^+$ ions have been found to act as particularly efficient proton-donating cations, various alternative candidates might at least be as equally efficient in affording well-ordered, insoluble assemblies with architectures notably different from that of **2a**.

Experimental Section

General methods: Manipulation under an inert gas atmosphere was not necessary. Infrared spectra were obtained on a Perkin–Elmer IR-1720 spectrometer supplemented with a noncommercial low-temperature device[24] and Raman spectra on a Jobin Yvon U-1000 equipped with a 514 nm Ar laser. Optical (NIR/VIS) absorption spectra were recorded on a Cary 5E instrument, and solution NMR spectra either on a Varian Gemini 200BB (^{1}H) or on a Bruker AM360 spectrometer (^{119}Sn). Room temperature magnetic susceptibilities were determined by means of Evans' method on a Johnson Matthey Chemicals susceptometer, and TG/DTG on a Netzsch STA 409 instrument. MS measurements were made on a Varian 331 A mass spectrometer and electrical conductivity measurements were conducted as described in ref. [5]. X-ray powder diffractograms were obtained on a Philips PW 1050 instrument ($Cu_{K\alpha}$ source and Ni filter), while the single-crystal X-ray study was performed on a Syntex $P2_1$ four-circle diffractometer.

The solid-state NMR spectra were recorded on a Varian VXR300 spectrometer operating at frequencies of 75.4, 111.9, 30.4, and 71.1 MHz for ^{13}C, ^{119}Sn, ^{15}N, and ^{59}Co, respectively. Cross-polarization with high-power proton decoupling was used for all spectra except ^{59}Co where direct polarization was used. The ^{13}C and ^{15}N spectra were recorded with a Doty Scientific probe with 7 mm o.d. rotors but for the ^{119}Sn and ^{59}Co spectra a faster-spinning Doty Scientific probe with 5 mm o.d. rotors was used. Acquisition conditions are given in the figure captions. Chemical shifts are reported, with the high-frequency positive convention, in ppm relative to the signals for $SiMe_4$, $SnMe_4$, NH_4NO_3 (nitrate line), and $K_3[Co(CN)_6]$(aq.) for ^{13}C, ^{119}Sn, ^{15}N, and ^{59}Co respectively.

Preparation of 2a–2f (see Table 1):

*Representative description of route A (coprecipitation) for **2b***: A solution of nBu$_4$NBr (160.5 mg, 0.50 mmol) and $K_3[Co(CN)_6]$ (165.5 mg, 0.50 mmol) in H_2O (10 mL) was added with stirring to a solution of Me_3SnCl (297.7 mg, 1.49 mmol) in H_2O (5 mL). After a reaction period of 10 h, the mixture was filtered and washed with a small portion of H_2O (twice). The white residue was dried in vacuo to afford analytically pure **2b**. Yield: 200 mg (50%).

*Representative description of route B ("remodeling") for **2b***: Pure $[(Me_3Sn)_3Co(CN)_6]$ (**1b**,[1] 140 mg, 0.43 mmol) was suspended in a solution of $[n\text{Bu}_4\text{N}][BF_4]$ (300 mg, 0.43 mmol) in H_2O (20 mL). The mixture was stirred for 15 h, filtered, washed with small portions of H_2O (twice), and dried in vacuo to afford pure **2b** (204 mg, 254 mmol, 60% yield). Alternatively, $[n\text{Bu}_4\text{N}]$OH was dissolved in CH_3OH instead of H_2O (ca. 25%).

2a: Anal. calcd for $C_{28}H_{56}N_7OFeSn_2$ (800.03): C 42.04, H 7.05, N 12.26, O 2.00, Fe 6.98; found C 41.71, H 7.01, N 12.11, O 2.00, Fe 6.92%. **2b**: anal.

calcd for $C_{28}H_{56}N_7OCoSn_2$ (803.12): C 41.87, H 7.03, N 12.21, O 1.99; found C 41.68, H 7.00, N 12.18, O 1.94%. **2c**: anal. calcd for $C_{28}H_{56}N_7OFePb_2$ (977.05): C 34.42, H 5.78, N 10.03; found C 33.93, H 5.67, N 9.90%. **2d**: anal. calcd for $C_{28}H_{56}N_7OCoPb_2$ (980.14): C 34.31, H 5.76, N 10.00, O 1.63; found C 33.41, H 5.51, N 9.78, O 1.60%. **2e**: anal. calcd for $C_{24}H_{50}N_7O_2FeSn_2$ (755.92): C 37.83, H 6.61, N 12.87, O 4.20; found C 37.49, H 6.56, N 12.79, O 4.10%. **2f**: anal. calcd for $C_{24}H_{50}N_7O_2CoSn_2$ (765.06): C 37.68, H 6.59, N 12.82; found C 37.48, H 6.57, N 12.69%.

X-ray crystallography: Single crystals of **2a** suitable for X-ray crystallography were recovered after 3–4 days from the filtrate obtained during the synthesis (vide supra) of **2a**. Crystal data for **2a**: $C_{28}H_{56}N_7OFeSn_3$, $M_r = 800.03\ g\,mol^{-1}$, triclinic, $P\bar{1}$, $a = 14.242(2) \times 10^2$, $b = 17.686(3) \times 10^2$, $c = 26.128(6) \times 10^2$ pm, $\alpha = 80.24(2)^\circ$, $\beta = 74.17(2)^\circ$, $\gamma = 78.207(14)^\circ$; $V = 6153(2) \times 10^6\ pm^3$, $Z = 6$, $\rho_{calcd} = 1.295\ g\,cm^{-3}$, $F(000) = 2442$. $T = 293(2)$ K, Θ-range: 2.30–25.05°; 21728 reflections independent of symmetry (total: 23039) for $R(int) = 0.0491$; data/restraints/parameters: 21721/0/1049, structure solution SHELX (SHELXTL PLUS(VMS), V4.2), refinement against F^2 with $R1 = 0.0608$ and $wR2 = 0.1494$ for $I > 2\sigma(I)$ (SHELXL-93); Powder diagram simulated with CERIUS^{2}3.0 (MSI), 2Θ range 5–50°. Further details of the crystal structure determination may be obtained from the Fachinformationszentrum Karlsruhe, D-76344 Eggenstein-Leopoldshafen (Germany) on quoting the depository number CSD 391055.

Acknowledgments: This work was supported by the Deutsche Forschungsgemeinschaft (Joint Project: Nanoporous Crystals) and the Fonds der Chemischen Industrie. Particular thanks are due to S. Samba for her technical assistance and to Professor U. Behrens for valuable advice on the crystallography. The extensive CPMAS NMR work was supported by the UK EPSRC (through the National Solid-State NMR Service based at Durham).

Received: October 31, 1997 [F872]

[1] U. Behrens, A. K. Brimah, T. M. Soliman, R. D. Fischer, *Organometallics* **1992**, *11*, 1718–1726.

[2] Me_3SnCl dissolved in H_2O (i.e. the $Me_3Sn \cdot aq^+$ ion) gives rise to one ^{119}Sn NMR signal at $\delta = +36.2$. This value is in good agreement with those reported for the $[Me_3Sn(OH_2)_2]^+$ ion in solid samples (see text and ref. [15]).

[3] P. Schwarz, S. Eller, E. Siebel, T. M. Soliman, R. D. Fischer, D. C. Apperley, N. A. Davies, R. K. Harris, *Angew. Chem.* **1996**, *108*, 1611–1614; *Angew. Chem. Int. Ed. Engl.* **1996**, *35*, 1525–1527.

[4] R. Tarhouni, Doctoral Dissertation, University of Hamburg (Germany), **1996**.

[5] P. Brandt, U. Illgen, R. D. Fischer, E. Sanchez-Martinez, R. Diaz Calleja, *Z. Naturforsch.* **1993**, *48b*, 1565–1573.

[6] In a similar manner, the coordination polymer $[(Me_3Sn)_4Fe(CN)_6]$ loses one mole of Me_3SnCN per formula unit in vacuo at $\approx 250\,^\circ C$ (ref. [4]).

[7] For this simplified consideration, symmetric vibrational modes resulting predominantly from *linear* NC-M-CN fragments have been ignored.

[8] For comparison, in the virtually nonpolymeric compound Me_3SnNCS the Sn–N distance is only 215 pm; see: R. A. Forder, G. M. Sheldrick, *J. Organomet. Chem.* **1970**, *21*, 115–122.

[9] See, for instance, refs. [1, 10–12, 20], and C. Carini, C. Pelizzi, G. Predieri, P. Tarasconi, F. Vitali, *J. Chem. Soc. Chem. Commun.* **1990**, 613–614.

[10] M. Adam, A. K. Brimah, R. D. Fischer, *Inorg. Chem.* **1990**, *29*, 1595–1597.

[11] U. Behrens, A. K. Brimah, R. D. Fischer, *J. Organomet. Chem.* **1991**, *411*, 325–330.

[12] A. Blaschette, D. Schomburg, E. Wieland, *Z. Anorg. Allg. Chem.* **1989**, *571*, 75–81.

[13] M. Witzel, B. Ziegler, D. Babel, *Z. Naturforsch.* **1988**, *43b*, 1311–1318; see also ref. [20].

[14] E. Siebel, P. Schwarz, R. D. Fischer, *Solid State Ionics* **1997**, *101–103*, 285–295, and references therein.

[15] J. Kümmerlen, A. Sebald, *J. Am. Chem. Soc.* **1993**, *115*, 1134–1142.

[16] S. Eller, P. Schwarz, A. K. Brimah, R. D. Fischer, D. C. Apperley, N. A. Davies, R. K. Harris, *Organometallics* **1993**, *12*, 3232–3240.

[17] Only $[(Me_3Sn)_4M^{II}(CN)_6]$ systems are exceptional[16] in that their Me_3Sn propellers already stop rotating slightly below room temperature. See also: R. K. Harris, M. Sünnetçioglu, R. D. Fischer, *Spectrochim. Acta* **1994**, *50A*, 2069–2078.

[18] Interestingly, the extra ^{15}N resonances were practically absent at $\approx -40\,^\circ C$. See: P. Schwarz, Doctoral Dissertation, University of Hamburg (Germany), **1994**, p. 24.

[19] J.-U. Schütze, R. Eckhardt, R. D. Fischer, D. C. Apperley, N. A. Davis, R. K. Harris, *J. Organomet. Chem.* **1997**, *534*, 187–194.

[20] P. Schwarz, E. Siebel, R. D. Fischer, C. D. Apperley, N. A. Davies, R. K. Harris, *Angew. Chem.* **1995**, *107*, 1311–1313; *Angew. Chem. Int. Ed. Engl.* **1995**, *34*, 1197–1199.

[21] J. Liu, W. T. A. Harrison, A. J. Jacobson, *Inorg. Chem.* **1996**, *35*, 4271–4273.

[22] M. Carcelli, C. Ferrari, C. Pelizzi, G. Pelizzi, G. Predieri, C. Solinas, *J. Chem. Soc. Dalton Trans.* **1992**, 2127–2128.

[23] P. Schwarz, Diploma Thesis, University of Hamburg (Germany), **1989**.

[24] The low-temperature device was constructed by Professor H.-D. Amberger (Hamburg).

  0947-6539/98/0405-0926 $ 17.50+.50/0 *Chem. Eur. J.* **1998**, *4*, No. 5